SMALL-X BEHAVIOUR OF NON-SINGLET STRUCTURE FUNCTIONS

B. I. Ermolaev*
Petersburg Physical-Technical Institute,
St.Petersburg, 194021, Russia,
S. I. Manayenkov †, M. G. Ryskin‡

Petersburg Nuclear Physics Institute,
Russian Academy of Science,
Gatchina, St.Petersburg district, 188350, Russia

Abstract

The small x behaviour of the non-singlet structure function is studied within the double logarithmic approximation (DLA) of perturbative QCD. Since there is neither k_T nor θ ordering in the ladder Feynman graphs, the predicted non-singlet quark densities for the HERA kinematical range ($x \sim 10^{-3}$) exceed the values calculated from the small-x approximation of the conventional Altarelli-Parisi evolution by a factor up to ten.

*This work was supported in part by the grant R26000 from the International Science Foundation and in part by Volkswagen Stiftung

†This work was supported in part by the Soros grant awarded by International Science Foundation

‡This work was supported in part by the grant INTAS-93-0079

1 INTRODUCTION

The small x behaviour of the non-singlet structure functions in deep inelastic scattering plays an important role for the precise description of the quark densities. Indeed, in order to check the Gottfried sum rule or to estimate the fraction of the initial nucleon spin carried by the quark (the spin crisis problem) one has to extrapolate the data into the small x region, and therefore one has to know the behaviour of the structure functions at small x.

The kinematical region $x \ll 1$ is of the Regge type, hence there are two possibilities for its investigation:

(i) to use conventional phenomenological formulae of the Regge type for the structure function description at the hadron level (see e.g. [1] and references therein);

(ii) within the framework of the perturbative QCD, to calculate and sum up the Feynman graphs yielding the leading contributions to the structure functions at the partonic level.

In the latter case one should take into account the Feynman graphs to all orders in the coupling constant for $x \ll 1$. The most popular way to carry this out consists of extrapolating (see e.g. [2], [3], [4], [5]) the Altarelli-Parisi equations, which describe DGLAP evolution of the structure functions with respect to $\ln(Q^2)$ [6], [7], [8] into the region $x \ll 1$. This equation sums up in the region $x \sim O(1)$ all the leading contributions coming from the Feynman graphs of the ladder type for the kinematical region where the transverse momenta k_{jT} of virtual partons (quarks and gluons) are strongly ordered

$$k_{nT} \ll \ ... \ \ll k_{2T} \ \ll \ k_{1T} \ll \sqrt{Q^2}. \tag{1}$$

The quantity $Q^2 = -q^2 > 0$ denotes the square of the photon mass.

Indeed, it has been proven in [8] that an integration over k_j in the region (1) yields the main contribution to the singlet and non-singlet structure functions at $x \sim O(1)$.

However, such ordering is not valid for summing up the leading contributions when $x \ll 1$. In this case the well known result [1] is that the condition (1) should be replaced by the ordering of the longitudinal Sudakov variables α_i, β_i for momenta k_i as follows:

$$\begin{aligned} \alpha_n \ll \ ... \, \alpha_2 \ll \ \alpha_1 \ll 1, \\ 1 \gg \beta_n \gg \ ... \ \gg \beta_1. \end{aligned} \tag{2}$$

Integration over k_i in the region (2) yields the leading contributions to the structure functions, in particular, the double-logarithmic (DL) contributions for the non-singlet structure functions (NSSF). Thus, one can evaluate NSSF by the direct calculation of the Feynman graphs of the ladder type. However there is another, simpler way to do this, namely, to make use of the Infrared Evolution Equation (IREE) for NSSF, i.e. of the evolution equation with respect to the infrared cut-off in the transverse momentum space. This method has first been applied in [11] to the description of the elastic scattering of quarks, and it has then been generalized to the investigation of inelastic scattering in

[1] Firstly, this result has been obtained in [9] for the investigation of the process $e^+e^- \to \mu^+\mu^-$ in QED. See also the review [10].

QED and QCD (see [11], [12], [13] and references therein). On the whole, this method has turned out to be an efficient way to calculate scattering amplitudes at high energies.

In the present paper we calculate the non-singlet structure functions in the double-logarithmic approximation (DLA) by constructing and solving both the integral equation of the Bethe-Salpeter type and IREE for it. In contrast to calculations based on extrapolating the conventional DGLAP into the region $x \ll 1$, we take into account not only the contributions $\sim \alpha_s^n \ln^{n-1}(x) \ln^n(Q^2)$ but also all the DL-contributions $\sim \alpha_s^n \ln^{n+k-1}(x) \ln^{n-k}(Q^2)$ for $k = 0,\ 1,\ ...,\ n$ in every order in α_s. The terms for $k = n$ become most important at very small x.

The paper is organized as follows. In Section 2 we review the main features of calculating Feynman graphs in DLA. We derive the linear integral equation for NSSF, taking into account the running QCD coupling constant $\alpha_s(Q^2)$ within DLA. In Section 3 we construct and solve IREE for NSSF. Here we assume α_s to be fixed. The solution is given in terms of the Mellin transformation. In Section 4 we discuss our results for fixed coupling constant and compare them with the conventional expression for NSSF obtained with Altarelli-Parisi evolution equation. In Section 5 we present numerical solutions of the integral equation for running QCD coupling and discuss a behaviour of the non-singlet structure functions at small x. We summarize our results in the Conclusion.

2 INTEGRAL EQUATION FOR THE NON-SINGLET STRUCTURE FUNCTION

In this section we give the outline of the Feynman graph calculation in DLA developed firstly in [9] (see also the review [10]) for the forward $e^+e^- \to \mu^+\mu^-$ scattering in QED and use it for constructing the integral equation for the non-singlet structure function $f_{NS}(x, Q^2)$ ($f_{NS} \equiv q_{n.s.}(x, Q^2)$) in deep inelastic lepton-nucleon scattering (DIS) at small x. In the framework of the perturbative QCD f_{NS} is given by the graph in Fig. 1 where the dashed lines correspond to the virtual photon with momentum q and the straight lines correspond to the quarks. The wavy lines we assign for gluons. The blob in Fig. 1 means that the radiative corrections in DLA are taken into account. The dotted line crossing the blob means that the intermediate s-channel particles are on-shell. We investigate f_{NS} in the kinematical region

$$\mu^2 \ll Q^2 \ll 2pq \tag{3}$$

i.e. at small x, where $x = Q^2/2pq$, p denotes the initial quark momentum and μ is the infrared cut-off. The leading (the double-logarithmic) contributions to f_{NS} come from the ladder Feynman graphs (Fig. 2). Let us remind that the structure function we consider here corresponds to the positive signature. Therefore non-ladder graphs, though yield DL-contributions, do not contribute to f_{NS} because they compensate each other totally. The reason for such a compensation in QCD and QED is that all non-ladder gluons are nearly on-shell and can be treated like the bremsstrahlung in the forward scattering, cancelling each other due to the destructive interference.

Thus, DL-contributions to the non-singlet structure function come from the ladder Feynman graphs in Fig. 2 only. To evaluate them, one should solve the linear integral equation in Fig. 3. for the sum of DL-corrections, A, to the elastic forward quark-antiquark scattering amplitude $A(t,\beta)$ (see Fig. 3):

$$A(t,\beta) = \int\limits_{\beta}^{1} \frac{d\beta'}{\beta'} \int\limits_{\mu^2}^{t_{max}} \frac{dt'}{t'} A(t',\beta') \frac{C_F}{2\pi} \alpha_s(t_{max}) + A_0, \tag{4}$$

where α_s is the QCD-coupling constant, $C_F = (N^2-1)/2N$ for the colour group SU(N). We have used in (4) the Sudakov parameterization for k in the following form

$$k = -\alpha q' + \beta p + k_T, \quad -k_T^2 \equiv t > 0, \tag{5}$$

where

$$q'_\mu = q_\mu - \frac{q^2 p_\mu}{2pq}\ , \tag{6}$$

and the analogous parameterization for k'. The nonhomogeneous term, A_0, in (4) is

$$A_0(t,\beta) = 4\pi C_F \alpha_s(t/\beta). \tag{7}$$

The limits in the integral over β' in (4) corresponds to the β-ordering (see e.g. [10]):

$$\beta' > \beta\ . \tag{8}$$

The lower limit in the integral over t' is given by some infrared cut-off μ, originated by applicability of the perturbative QCD to the problem , while the upper one t_{max} comes from the condition $k_{\|}^2 \equiv \alpha\beta s \leq \mid t \mid$ (where $s \equiv 2pq$). Indeed, if $k_T' \gg k_T$ the value of α in (5) is $\alpha \approx -(k_T - k_T')^2/\beta' s \approx t'/s\beta'$ and, when $t' > t\beta'/\beta$, the longitudinal part of $k_{\|}^2$ becomes so large,

$$k_{\|}^2 = s\alpha\beta \sim t'\beta/\beta' \geq t, \tag{9}$$

that it destroys the logarithmic structure of the integrand dt'/t' in (4) (see [10] for the details).

So, within the DLA we put

$$t_{max} = t\beta'/\beta\ . \tag{10}$$

Let us notice that for small x (i.e. when $\beta' \gg \beta$) this value is larger than the upper limit when $t_i = k_{iT}^2$ are ordered (see (1)). Now let us show that the argument of the QCD coupling constant in (4) is also equal to t_{max}. To find it, one has to consider the quark loop inserted into the gluon propagators in Fig. 2 (see also Fig. 3). The integral over the invariant mass of the loop looks as $\int dM^2/M^2$. This logarithmical behaviour continues up to $M^2 \sim t_{max} = t\beta'/\beta$ where the large value of M^2 corresponds again to the essentially large $k_{\|}^2 \sim M^2\beta/\beta' \sim t$. Thus, the argument of α_s should be t_{max} [2].

[2]Note that for small x (i.e. when $\beta' \gg \beta$) this value is much greater than the argument in the canonical Altarelli-Parisi equation ($t_{max} = t$).

Finally, to obtain the non-singlet structure function, f_{NS}, we integrate A over t:

$$f_{NS}(x,Q^2) = \delta(1-x) + \frac{1}{8\pi^2}\int\limits_{\mu^2}^{s_{max}} A(t,\beta)\frac{dt}{t} \ , \tag{11}$$

with $s_{max} = s/4$ and

$$\beta = x + t/s \ . \tag{12}$$

Here the upper limit, $s/4$, is fixed formally by the kinematics, but, in reality, the bulk of integration in (11) is determined by dependence on β. At $t \gg Q^2$, the term t/s increases the value of β crucially, and as the amplitude $A(t,\beta)$ falls down with an increase of β the essential value of t in equation (11) is of the order of Q^2. It should be noticed that the expression (11) corresponds to the integration with the transversely polarized photon i.e. to σ^T. In the case of the longitudinal heavy photons one has to write, in the denominator, Q^2 instead of t

$$\frac{\sigma^L}{\sigma^T} = \frac{\int\limits_{\mu^2}^{s_{max}} A(t,\beta)dt/t}{\int\limits_{\mu^2}^{s_{max}} A(t,\beta)dt/Q^2}, \tag{13}$$

where β in (13) is given by (12).

3 IREE FOR THE NON-SINGLET STRUCTURE FUNCTION

In this section we construct and solve the evolution equation for NSSF with respect to the infrared cut-off in the transverse momentum space. It is more convenient to consider, instead of the non-singlet structure function, f_{NS}, the scattering amplitude, M, for the forward quark-photon scattering where photon is off-shell (see Fig. 4). The Optical theorem gives the simple relation between f_{NS} and M.

Indeed,

$$2\pi^2\alpha e_q^2\frac{tr\{\hat{p}\hat{e}(\hat{p}+\hat{q})\hat{e}\}}{(2pq)^2}f_{NS} = \frac{1}{s}ImM \tag{14}$$

where e_μ is the photon polarization vector and α is the QED coupling constant. e_q in (14) denotes the electric charge of the initial quark. As we are discussing the forward scattering, the amplitude M depends on s, Q^2 and on the masses of quarks taken into account.

There are graphs with the ultraviolet and the infrared singularities among the Feynman graphs contributing to M. We can easily avoid the problem of the ultraviolet singularities by noticing that we will treat any single Feynman graph contribution to M as the result obtained with the dispersion relations from its imaginary part (with respect to s) which has not the ultraviolet singularities. In order to get rid of the infrared singularity problem, one should introduce some infrared regularization. Let us define the infrared cut-off parameter, μ:

$$\mu \ll k_{iT}, \quad i = 1,\ 2, ... \tag{15}$$

where k_{iT} denotes the momentum of virtual particle i (a quark or gluon), transverse to the plane formed by momenta p and q' (see (5)):

$$pk_{iT} = q^{'}k_{iT} = 0. \tag{16}$$

Such a regularization does not destroy the gauge invariance, so we can fix any gauge for the virtual gluons at convenience. In the present paper we use the Feynman gauge.

It was shown in [12] that μ, being the minimal transverse momentum, also place the role of a new mass scale. Thus, we can neglect masses of the virtual quarks and be free of the infrared singularities in the same time. In DLA, the value of μ can be chosen much greater than Λ_{QCD}.

As M now depends on s, Q^2, and on the new mass scale μ, in the form

$$M = M(s/\mu^2, Q^2/\mu^2), \tag{17}$$

one can differentiate it with respect to μ. Let us notice that

$$-\mu^2\frac{\partial M}{\partial \mu^2} = \frac{\partial M}{\partial z} + \frac{\partial M}{\partial y} \tag{18}$$

where

$$z = \ln(s/\mu^2), \quad y = \ln(Q^2/\mu^2). \tag{19}$$

Expression (18) is the left-hand side of the IREE for M (the left-hand side of the equation in Fig. 5).

Now let us obtain the right-hand side of the IREE. First of all, let us notice that the ordering conditions (8) do not mean the ordering for t_i in the ladder Feynman graphs. Indeed, integration of such graphs over α_i yields (see [10])

$$t_n/\beta_n \ll \cdots \ll t_2/\beta_2 \ll t_1/\beta_1. \tag{20}$$

Since t_i are not ordered, integration over any of t_i gets μ^2 as the lowest limit. On the other hand within the DLA all the momenta k_j are quite different from each other. If two of them (say, k_{iT} and k_{jT}) are of the same order one looses at least one logarithm. Thus, the region (20) can be considered as a superposition of the regions Ω_i where the transverse momenta k_{jT} are ordered (with respect to the absolute value of k_{jT} but not with respect to the index j). Let the minimal transverse momentum square in the region Ω_i be t_i. Therefore, in every such region Ω_i, μ is the lowest limit only for integration over k_{iT} whereas integration over other transverse momenta does not involve μ at all. In other words, the ladder Feynman graph (and therefore the sum of them) can be treated as a convolution of two ladder graphs, so that, in each the graph, integration over transverse momenta begins from t_i in the region Ω_i, i.e. for them k_{iT} takes place of μ, being a new infrared cut-off when the quark masses are neglected. Let us denote such a minimal transverse momentum as k_T. Ordering (20) means that the quark pair with the minimal k_T can be in any place of the ladder graph in Fig. 2. In the case of t_i-ordering the quarks with the minimal k_T would be in the fixed place of the ladder graph (in the bottom of the graph in Fig. 2).

Thus, beyond the Born approximation, the amplitude M can be represented as the convolution of two amplitudes (the last term in the right-hand side of the equation in Fig. 5). The first of these amplitudes is the same amplitude M with replacement μ by k_T and s by $2kq$. The second one is the amplitude M_0 for the forward quark-antiquark scattering.

Adding the Born amplitude M_B to the right-hand side of the equation, we obtain the equation in Fig. 5 for f_{NS} in the graphic form. This equation can be easily rewritten in the analytic form in the momentum space with using the standard Feynman rules.

It is convenient however, to perform the Sommerfeld-Watson transformation which partly coincides with the Mellin transformation :

$$M(z,y) = \int\limits_{\lambda-i\infty}^{\lambda+i\infty} \frac{d\omega}{2\pi i}(s/\mu^2)^\omega F(\omega,y) \tag{21}$$

where λ is chosen so that the integration contour in (21) was on the right of the singularities of F. The variable ω corresponds to the angular momentum in the complex momentum plane. Having performed the Mellin transformation, we obtain the equation for F in the following simple form: [3]

$$\omega F + \frac{\partial F}{\partial y} = \frac{1}{8\pi^2} f_0(\omega) F \tag{22}$$

where f_0 is the Mellin amplitude for the forward scattering of on-shell quarks in DLA [11]. There is not a contribution coming from the Born amplitude M_B in (22) because M_B does not depend on μ in the region (2).

As equation (22) is linear, one can easily obtain its solution:

$$F = \Phi(\omega)\exp\{(-\omega + f_0/8\pi^2)y\} \ . \tag{23}$$

$\Phi(\omega)$ in (23) should be specified with a certain boundary condition. Let us fix it at the point $y = 0$:

$$F(\omega,y)\mid_{y=0} = \Phi(\omega). \tag{24}$$

Thus, in order to specify Φ we should construct and solve IREE for the amplitude of quark-photon forward scattering, $\tilde{M}$, where the photon is (nearly) on-shell. Immediately we obtain for its Mellin amplitude, $\tilde{F}(\omega)$, similar equation:

$$\omega\tilde{F} = C_0 + \frac{1}{8\pi^2} f_0(\omega)\tilde{F}(\omega) \ , \tag{25}$$

$$C_0 = \frac{-\pi\alpha e_q^2 tr\{\hat{p}\hat{e}(\hat{p}+\hat{q})\hat{e}\}}{pq} \ . \tag{26}$$

The first term in the right-hand side of (25) is the contribution of the Born graph which depends on μ when $y = 0$.

Solution of (25) gives us

$$\tilde{F} = C_0/(\omega - f_0/8\pi^2). \tag{27}$$

[3]For details of the method see [11], [12], [13] and the references therein.

The Mellin amplitude $f_0(\omega)$, firstly obtained in [11], satisfies the same differential equation like $\tilde{F}(\omega)$ with obvious replacements $\tilde{F}$ by f_0 in equation (25) and C_0 by a_0,

$$a_0 = g^2 C_F \tag{28}$$

where g is the QCD-coupling constant. Thus, the equation

$$\omega f_0 = a_0 + f_0^2/(8\pi^2) \tag{29}$$

for f_0 is non-linear, though very simple. Its solution is

$$f_0 = 4\pi^2\omega[1 - \sqrt{1 - a_0/(2\pi^2\omega^2)}] \tag{30}$$

where the sign minus before the square root sign was chosen so that

$$f_0 \mid_{\omega \gg 1} \sim a_0/\omega \tag{31}$$

where a_0/ω is the Born approximation for f_0. Equation (29) permits to simplify (27) because it gives

$$\omega - f_0/(8\pi^2) = a_0/f_0 \ . \tag{32}$$

Thus, combining (29), (27) and (23), we obtain

$$F(\omega, y) = \frac{C_0}{g^2 C_F} f_0(\omega) \exp\{-[\omega - f_0/(8\pi^2)]y\}. \tag{33}$$

It leads to

$$M(\frac{s}{\mu^2}, \frac{Q^2}{\mu^2}) = \frac{C_0}{g^2 C_F} \int\limits_{\lambda - i\infty}^{\lambda + i\infty} \frac{d\omega}{2\pi i} \Big(\frac{s}{Q^2}\Big)^{\omega} f_0(\omega) \exp\{y f_0(\omega)/(8\pi^2)\}. \tag{34}$$

With using (14) and the fact that in DLA

$$Im M \approx -\pi dM/d\ln(s) \tag{35}$$

we obtain for the non-singlet structure function the following expression

$$f_{NS} = \frac{1}{g^2 C_F} \int\limits_{\lambda - i\infty}^{\lambda + i\infty} \frac{d\omega}{2\pi i} \Big(\frac{s}{Q^2}\Big)^{\omega} \omega f_0(\omega) (Q^2/\mu^2)^{f_0(\omega)/(8\pi^2)} \ . \tag{36}$$

4 PROPERTIES OF THE SOLUTION OF THE IREE

The expression (36) for the non-singlet structure function takes into account DL contributions to all orders in the coupling constant, and therefore can be represented as an expansion in powers of α_s. In terms of the Mellin variable ω, we can consider the expansion of f_0 into a power series in $1/\omega$ and integrate the result over ω according to

$$\int \frac{d\omega}{2\pi i} (\frac{1}{x})^{\omega} \omega^{-k-1} = \frac{1}{k!} \ln^k(\frac{1}{x}), \tag{37}$$

$k = 1,\ 2, \cdots$.

As

$$f_0 \approx 4\pi^2(\frac{a}{2\omega} + \frac{a^2}{8\omega^3} + \frac{a^3}{16\omega^5}) + O(\omega^{-7}), \tag{38}$$

with $a = 2\alpha_s C_F/\pi$, we obtain from (36)

$$f_{NS} \approx \frac{4\pi^2}{g^2 C_F}\int \frac{d\omega}{2\pi i}\Big(\frac{1}{x}\Big)^{\omega}\omega\Big(\frac{a}{2\omega} + \frac{a^2}{8\omega^3} + \frac{a^3}{16\omega^5}\Big)$$
$$\exp\Big\{y[\frac{a}{4\omega} + \frac{a^2}{16\omega^3} + \frac{a^3}{32\omega^5}]\Big\}\ . \tag{39}$$

It should be stressed that for the non-singlet function at small x one deals with the expansion $(\alpha_s/\omega^2)^k$, which is much more singular (at $\omega \to 0$) than the expansion $(\alpha_s/\omega)^k$ typical for the singlet (BFKL-pomeron) case. Thus, the summation of the whole DL series becomes very important.

If $\omega \gg a$, one can neglect all terms in (39) proportional to $(a/\omega^2)^k$ $(k > 1)$, compared to the first one. It leads to the well known expression $\tilde{f}_{NS}$ for the non-singlet structure function:

$$f_{NS} \approx \tilde{f}_{NS} = \int\limits_{\lambda - i\infty}^{\lambda + i\infty} \frac{d\omega}{2\pi i}\Big(\frac{1}{x}\Big)^{\omega}\exp(\frac{ay}{4\omega}). \tag{40}$$

Expression (40) is obtained from the conventional Altarelli-Parisi evolution equation which is valid in the region $x \sim 1$ where it correctly sums up all the leading $\ln Q^2$ contributions to f_{NS}, by retaining in the anomalous dimension only the singular part in $1/\omega$. However, as it is clear from (39), it fails in the region $x \ll 1$, where DL-contributions, proportional to $\ln^{2k}(1/x)$ becomes extremely essential and therefore should not be neglected.

To demonstrate this let us expand (36) and (40) in inverse powers of ω and integrate them over ω with using (37). We obtain

$$f_{NS} = \delta(x-1) + \frac{a}{4}[\ln(1/x) + \ln(Q^2/\mu^2)] +$$
$$+\frac{a^2}{96}[2\ln^3(1/x) + 6\ln^2(1/x)\ln(Q^2/\mu^2) +$$
$$+3\ln(1/x)\ln^2(Q^2/\mu^2)] + O(a^3), \tag{41}$$

$$\tilde{f}_{NS} = \delta(x-1) + \frac{a}{4}\ln(Q^2/\mu^2) + \frac{a^2}{32}\ln(1/x)\ln^2(Q^2/\mu^2) + O(a^3). \tag{42}$$

Though the first, the Born terms, in (41), (42) coincide, higher loop corrections are quite different. Indeed, for the ratio of the first loop contributions (terms proportional to a) we obtain

$$r_1 = 1 + \frac{\ln(1/x)}{\ln(Q^2/\mu^2)}\ , \tag{43}$$

and for the ratio of the second loop contributions (terms proportional to a^2)

$$r_2 = 1 + \frac{2\ln(1/x)}{\ln(Q^2/\mu^2)} + \frac{2\ln^2(1/x)}{3\ln^2(Q^2/\mu^2)}. \tag{44}$$

If we put, for example,

$$\mu^2 = 0.1\ GeV^2,\ Q^2 = 20\ GeV^2 \text{ and } x = 10^{-3}, \tag{45}$$

we obtain

$$r_1 \approx 2.3,\ \ r_2 \approx 4.7. \tag{46}$$

Thus, being equal in the Born approximation, f_{NS} and the conventional non-singlet structure function $\tilde{f}_{NS}$ differ a lot when the radiative corrections are taken into account. This difference increases with the order of perturbation expansion.

Now let us estimate the ratio $f_{NS}/\tilde{f}_{NS}$ at small x, using their asymptotic expressions. With the standard technique (the saddle point method), we find that at $by \gg 1,\ y \gg \rho$

$$\tilde{f}_{NS} = \sqrt{\frac{b}{8\pi}}\Big(\frac{y}{\rho^3}\Big)^{1/4}\exp(b\sqrt{y\rho}) \tag{47}$$

where we have used the notations $\rho = -\ln(x),\ b = \sqrt{a},\ y = \ln(Q^2/\mu^2)$.

The asymptotic expression for f_{NS} at $b\rho \gg 1,\ by \gg 1$ is [4]

$$f_{NS} = \sqrt{\frac{b}{2\pi}}\frac{y(\rho + y/2)}{\rho^{3/4}(\rho + y)^{7/4}}\exp\{b\sqrt{\rho(\rho + y)}\}\ . \tag{48}$$

Thus, for the ratio we have

$$f_{NS}/\tilde{f}_{NS} = \frac{2y^{3/4}(\rho + y/2)}{(\rho + y)^{7/4}}\exp\{b(\sqrt{\rho(\rho + y)} - \sqrt{\rho y})\}\ . \tag{49}$$

For example, if we choose the same values (45) for $\mu^2,\ s,\ Q^2$ and put $\alpha_s = 0.3$, we obtain from (49) the estimate $f_{NS}/\tilde{f}_{NS} \approx 4.1$. More accurately, a numerical evaluation of f_{NS} and $\tilde{f}_{NS}$ given by (36) and (40) yields the following result:

$$r = f_{NS}/\tilde{f}_{NS} \approx 5.56\ . \tag{50}$$

Our results for other values of x and μ, with $Q^2 = 20\ GeV^2$, are presented in Table 1. The value of α_s for $\mu^2 = 0.1$ was put by hands equal to 0.3 whereas for other μ $\alpha_s = \alpha_s(\mu^2)$.

Table 1.

$\mu^2,\ GeV^2$	x	$r = f_{NS}/\tilde{f}_{NS}$	α_s
0.1	0.001	5.56	$0.3^\star$
0.1	0.01	2.94	$0.3^\star$
0.1	0.1	1.64	$0.3^\star$
1.0	0.001	10.26	0.394
1.0	0.01	4.52	0.394
1.0	0.1	2.10	0.394
4.0	0.001	12.71	0.283
4.0	0.01	5.94	0.283
4.0	0.1	2.75	0.283

[4] For $\rho \gg y$ and at $by \sim 1$ when the position of the saddle point ω_0 is close to the branching point of $f_0(\omega)$ ($\omega_0 \to b$) one should apply more precise formula $f_{NS} = \sqrt{2/\pi b}(1 + yb/2)\rho^{-3/2}\exp\{b\sqrt{\rho(\rho + y)}\}$.

In the Mellin representation, the Altarelli-Parisi equation for $\tilde{f}_{NS}$ can be written as

$$\frac{\partial \tilde{f}_{NS}}{\partial \ln(Q^2)} = [-\omega + \alpha_s C_F/(2\pi\omega)]\tilde{f}_{NS} \ . \tag{51}$$

IREE gives the Q^2-dependence of f_{NS} as:

$$\frac{\partial f_{NS}}{\partial \ln(Q^2)} = [-\omega + f_0(\omega)/(8\pi^2)]f_{NS}. \tag{52}$$

The first terms in the brackets in (51), (52) are not essential. They disappear if one uses the Mellin transformation in the form

$$M = \int \frac{d\omega}{2\pi i}\Big(\frac{s}{Q^2}\Big)^{\omega} F(\omega, Q^2) \tag{53}$$

instead of (21).

Thus, the only essential difference between (51) and (52) is the difference in the "kernels" in these equations. When $x \sim 1$, the replacement of f_0 by its Born value makes (52) coincide with (51). In a sense, the opposite replacement $\alpha_s C_F/(2\pi\omega)$ by $f_0(\omega)$ corresponds to taking into account all next-to-leading corrections of the type of $(\alpha_s/\omega^2)^n$ to the Altarelli-Parisi kernel. Being small in the region $\omega \sim 1$, they become large when $\omega \to 0$ ($x \to 0$). In this connection, let us notice that these corrections are proportional to $(\alpha_s/\omega^2)^k$ only due to the fact that integration over all transverse momenta yields large contributions from the region of small k_{iT} ($k_{iT} \geq \mu$). Hence, if one wants to take into account non-perturbative contributions to f_{NS} (see e.g. [4]), one has to consider them, besides the leading order, in the non-leading orders also.

Thus, in the present paper we have shown that the applicability of the conventional expression (40) for the non-singlet structure function at the small x region is quite doubtful. The standard and widespread Monte-Carlo programs (e.g. HERWIG and LEPTO) should be changed when they operate with the f_{NS} in the region $x \ll 1$. The main reason for the discrepancy is that in the Regge kinematical region $x \ll 1$, the transverse momenta of the virtual quarks in the ladder graphs are not ordered, in contrast to the transverse momentum ordering in the Altarelli-Parisi evolution at $x \sim 1$. It leads to replacement of expression (40) by f_{NS} given by (36).

Such an amendment leads to a drastic change of the asymptotic behaviour of the non-singlet structure function. Indeed, the conventional formula (40) leads to the behaviour for $x \to 0$

$$\tilde{f}_{NS} \sim \exp\Big\{\sqrt{\frac{2\alpha_s C_F}{\pi}\ln(Q^2/\mu^2) ln\frac{1}{x}}\Big\}, \tag{54}$$

while the IR evolution equation gives at $x \to 0$

$$f_{NS} \sim \exp\Big\{\Big(\sqrt{\frac{2\alpha_s C_F}{\pi}}\Big)\Big[\frac{1}{2}\ln(\frac{Q^2}{\mu^2}) + \ln(\frac{1}{x})\Big]\Big\} \ , \tag{55}$$

thus demonstrating the more singular behaviour of f_{NS} compared to $\tilde{f}_{NS}$ at small x. The growth of the non-singlet quark density can be written as

$$f_{NS} \sim x^{-\gamma} \ , \tag{56}$$

where $\gamma = d\ln f_{NS}/d\ln(1/x)$ is an effective power. One can see that, for $\tilde{f}_{NS}$, its value

$$\tilde{\gamma} = \sqrt{\frac{\alpha_s C_F}{2\pi}\frac{\ln(Q^2/\mu^2)}{\ln(1/x)}} \tag{57}$$

is smaller at very small x than γ from (55) which predicts

$$\gamma = \sqrt{2\alpha_s C_F/\pi}\ . \tag{58}$$

5 EFFECTS OF THE RANNING COUPLING ON f_{NS}

Table 1 shows that the numerical value of f_{NS} depends on the choice of the argument of α_s. Strictly speaking, in the framework of DLA we have used in the previous sections, α_s should be treated as the fixed one because the radiative corrections making it running are the single-logarithmic (SL) ones and therefore are beyond the DL-accuracy.

The consistent study of the effects on f_{NS} induced by the running coupling should include consideration of all possible SL-contributions to f_{NS}. However, here we restrict ourselves with consideration only a part of the SL-contributions, namely the SL-contributions arising from the running coupling. As we were not able to solve this problem by analytical calculation, we present below the numerical solutions of equation (4) within the HERA energy range. The results are presented in Fig. 6. To be unambiguous, let us remind that through the present paper (including the curves in Fig. 6) the quantity we call f_{NS} corresponds to the scattering on the isolated initial quark with momentum p. In order to obtain the non-singlet structure function, one should convolute that quantity with the initial quark distribution q_{NS}. However, as q_{NS} has no singularity in the region of small momenta, small x behaviour of the convolution and the one of f_{NS} coincides in the DLA.

As one can expect, the values of f_{NS}, when the coupling is running, are smaller compared to the ones for the fixed $\alpha_s = \alpha_s(\mu^2)$ and larger than that ones for $\alpha_s = \alpha_s(s/4)$. Numerically it is more close to the latter case as one can see from Fig. 7a. At $10(GeV/c)^2 \leq Q^2 \leq 300(GeV/c)^2$ and $0.0001 \leq x \leq 0.04$ the result can be approximated by the solution with the fixed coupling

$$\alpha_s = \alpha_s(Q^2) \tag{59}$$

with the effective Λ instead of the usual Λ_{QCD} given by the relation

$$\Lambda_{eff} = 0.2\ \Lambda_{QCD}\ x^{0.1}. \tag{60}$$

Figure 7b shows that these phenomenological formulae can be used for the estimation of f_{NS} with an accuracy better than 20%.

The effective power of γ describing the growth of the non-singlet quark distribution at small x is about 2 times smaller than that one for the fixed coupling ($\alpha_s = \alpha_s(\mu^2)$) case. Withing the HERA energy range f_{NS} can be described by (56) with $\gamma \approx 0.24$

(see Fig. 8). It is interesting to note that at small x ($x < 0.01$) the Q^2-dependence of γ looks quite opposite to the dependence predicted by straightforward extrapolating of the Altarelli-Parisi formulae into the small x region. Indeed, one can expect from (40), (54) that γ should increase with increase of $\ln(Q^2)$ (see (57)). In contrast to it, Fig. 8 demonstrates that larger values of γ correspond to smaller Q^2. It is explained by the fact that in (4) the terms $\sim \alpha_s^n(\ln(1/x)^{2n-1}$ become more important at small x than the terms $\sim \alpha_s^n(\ln(1/x))^{n-1}\ln^n(Q^2)$ which are taken into account by the Altarelli-Parisi equation. When Q^2 increases, the essential values of the argument of α_s also increase. Thus, at large Q^2 we deal with a smaller value of the coupling and get a smaller value for the effective power of γ. In the region $x \sim 1$ one can use the k_T-ordering typical for the standard Altarelli-Parisi equation. Here the main contribution to f_{NS} comes from the terms $\sim \alpha_s^n \ln^{n-1}(1/x)\ln^n(Q^2)$ (or for the running coupling $\sim (\ln(1/x))^{n-1}\left(\ln\frac{\ln(Q^2/\Lambda^2)}{\ln(\mu^2/\Lambda^2)}\right)^n$). So at larger x a larger power of γ corresponds to a larger virtuality Q^2 .

Another point we have to stress is a rather week Q^2-dependence of the quark distribution (f_{NS}) at small x. The reason is the same as above: at each order in α_s the term of the kind $\alpha_s^n(\ln(1/x))^{2n-1}$ is the dominant one while the $\alpha_s^n \ln^{2n-1-k}(1/x)\ln^k(Q^2)$ terms for $k \geq 1$ play the role of a correction only. As one can see from Fig. 6 the growth of $f_{NS}(x,Q^2)$ depends weekly on Q^2 and does not exceed 1.7 times within the interval $10 \leq Q^2 \leq 300(GeV/c)^2$ (5.5 times in the case of Altarelli-Parisi equation) at $x = 10^{-3}$. The Q^2-dependence of the effective power $\gamma(Q^2)$ at $x < 0.003$ is almost negligible (see Fig. 8). Thus, the parameterization of the non-singlet quark density in the form

$$f_{NS} = \Phi(Q^2)x^{-\gamma} \tag{61}$$

where only the pre-exponent factor Φ depends on Q^2 looks quite reasonable (at least as the first approximation) for the phenomenological purpose in the small x region. Contrary the Altarelli-Parisi prediction depends strongly on Q^2 (see (54)) and at not too large Q^2 the ratio $r(x)$ of the non-singlet structure function f_{NS} obtained with the aid of (4) and (11) to the Altarelli-Parisi one $\tilde{f}_{NS}$ shown in Fig. 9 increases crucially with $\ln(1/x)$.

6 CONCLUSION

So, in the present paper we have calculated the non-singlet structure function at small x available for HERA energy range. We have shown that in the double-logarithmic approximation (with the coupling fixed) the expression for f_{NS} considerable differs from the one obtained by extrapolating of the Altarelli-Parisi results into the region $x \ll 1$. The main reason for such a discrepancy is that the transverse momenta of virtual quarks in the ladder Feynman graphs are not ordered in small x region in contrast to the case of $x \sim 1$. When the coupling is running, the discrepancy is not so large. However, one can treat it as an indication to importance of studying the single-logarithmic contributions to f_{NS} as well.

ACKNOWLEDGEMENT

We are grateful to J.Bartels and to L.N.Lipatov for useful discussions. We would like to gratefully acknowledge the hospitality of the DESY Theory Group and the financial support of the Volkswagen Stiftung.

References

[1] F. E. Close, R. G. Roberts: *Phys. Lett.* **B316** (1993) 165;
S. Forte: *Preprint CERN-TH* **7453/94**;
P. Amaudruz et al.: *Phys. Rev. Lett.* **66** (1991) 2712;
R.L.Heiman: *Nucl. Phys.* **B64** (1973) 429.

[2] G. Ingelman: "Physics at HERA" edited by W. Buchmüller, v. 3, p. 1366; Hamburg, 1991.

[3] G. Marchesini, B. R. Webber: *Nucl. Phys.* **B310** (1988) 461;
B. R. Webber: "Physics at HERA" edited by W. Buchmüller,
G. Ingelman: v. 3, p. 1354; Hamburg, 1991.

[4] S. Forte and R. D. Ball: *Preprint CERN-TH* **7436/94**.

[5] F. E. Close, R. G. Roberts: *Phys. Lett.* **B336** (1994) 257.
F. E. Close, R. G. Roberts: *Preprint RAL-94-071.*

[6] V. N. Gribov and L. N. Lipatov: *Sov. Journ. Nucl. Phys.* **15** (1972) 438 and 675.

[7] G. Altarelli and G. Parisi: *Nucl. Phys.* **126** (1977) 297.

[8] Yu. L. Dokshitser: *Sov. Phys. JETP* **46** (1977) 641.

[9] V. G. Gorshkov,V. N. Gribov, L. N. Lipatov and G. V. Frolov: *Sov. J. Nucl. Phys.* **6** (1967) 95.

[10] V.G.Gorshkov: *Sov. Phys. Uspekhi* **16** (1973) 322.

[11] R. Kirschner and L. N. Lipatov: *Nucl. Phys.* **B213** (1983) 122.

[12] B. I. Ermolaev and L. N. Lipatov: *Int. J. Mod. Phys.* **A4** (1989) 3147.

[13] B. I. Ermolaev: *Z. Phys.* **C65** (1995) 299.

Figure captions

Fig. 1. Graph for f_{NS}. The blob indicates that the radiative corrections in DLA are taken into account.

Fig. 2. Graph of the ladder type for f_{NS}. Crosses on the lines mark on-shell intermediate particles.

Fig. 3. Equation of the Bethe-Salpeter type for $A(t,\beta)$.

Fig. 4. The amplitude M (μ denotes the infrared cut-off).

Fig. 5 The evolution equation for M and $\tilde{M}$.

Fig. 6. Quark distributions f_{NS} at small x. Curves are obtained with the aid of (4) and (11) for running coupling at $\mu^2 = 4\ (GeV/c)^2$ and $\Lambda_{QCD} = 200\ MeV/c$.

Fig. 7a. Quark distributions f_{NS} at $Q^2 = 100\ (GeV/c)^2$. Solid and dotted curves have been obtained for constant coupling for $\alpha_s = \alpha_s(\mu^2)$ and $\alpha_s = \alpha_s(s/4)$, respectively. Dashed curve corresponds to running coupling. Parameters μ^2 and Λ_{QCD} are as for Fig. 6.

Fig 7b. Ratios of non-singlet structure functions. Curves show ratios of f_{NS} obtained for constant coupling with Λ_{eff} given by (60) to solution of equation (4) for running coupling. Parameters μ^2 and Λ_{QCD} are as for Fig. 6.

Fig. 8. Effective power of γ. Curves present $\gamma = d\ln(f_{NS})/d\ln(1/x)$ for solution of integral equation (4) for running coupling at $\mu^2 = 4\ (GeV/c)^2$ and $\Lambda_{QCD} = 200\ MeV/c$.

Fig. 9. Ratios of structure functions for running coupling. Curves present ratios $r(x)$ of f_{NS} calculated with the aid of (4) and (11) to Altarelli-Parisi structure functions $\tilde{f}_{NS}$. Parameters μ^2 and Λ_{QCD} are as for Fig. 6.

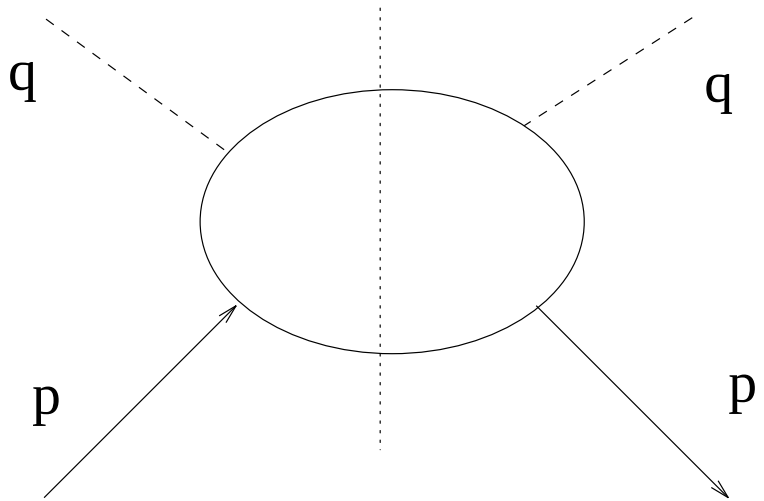

Fig. 1

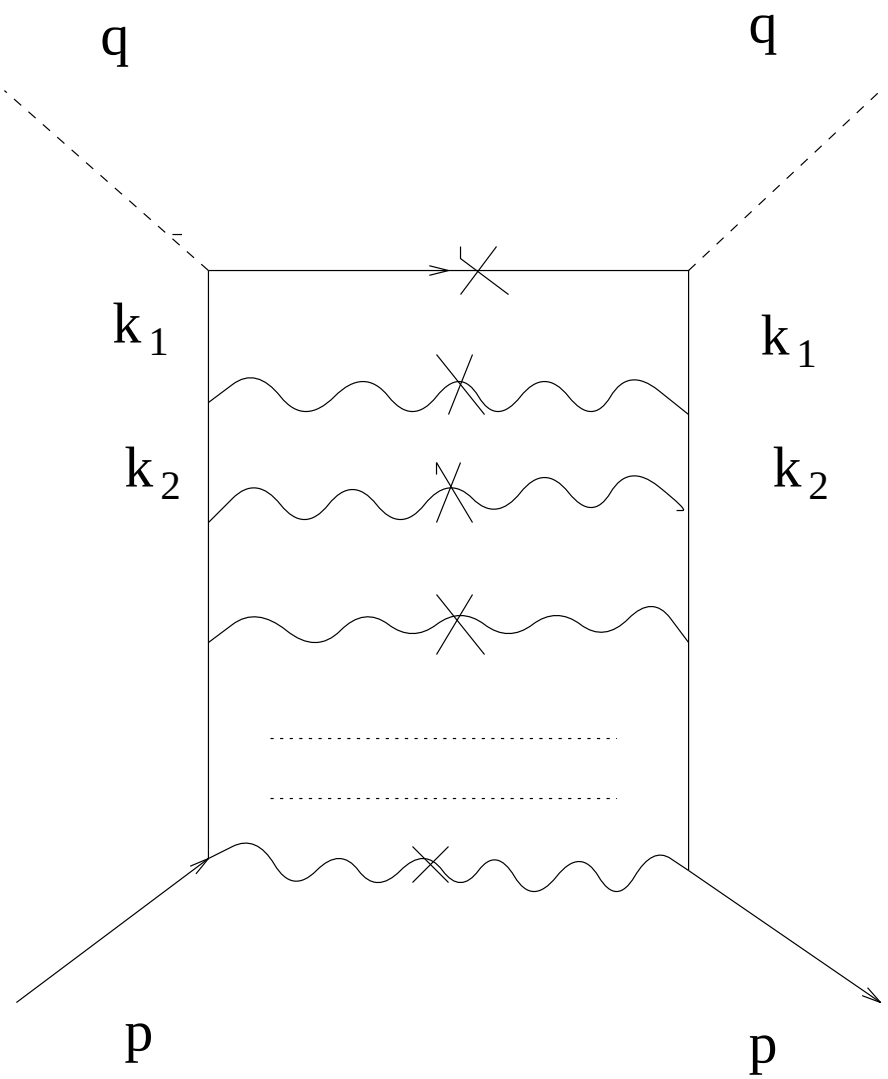

Fig. 2

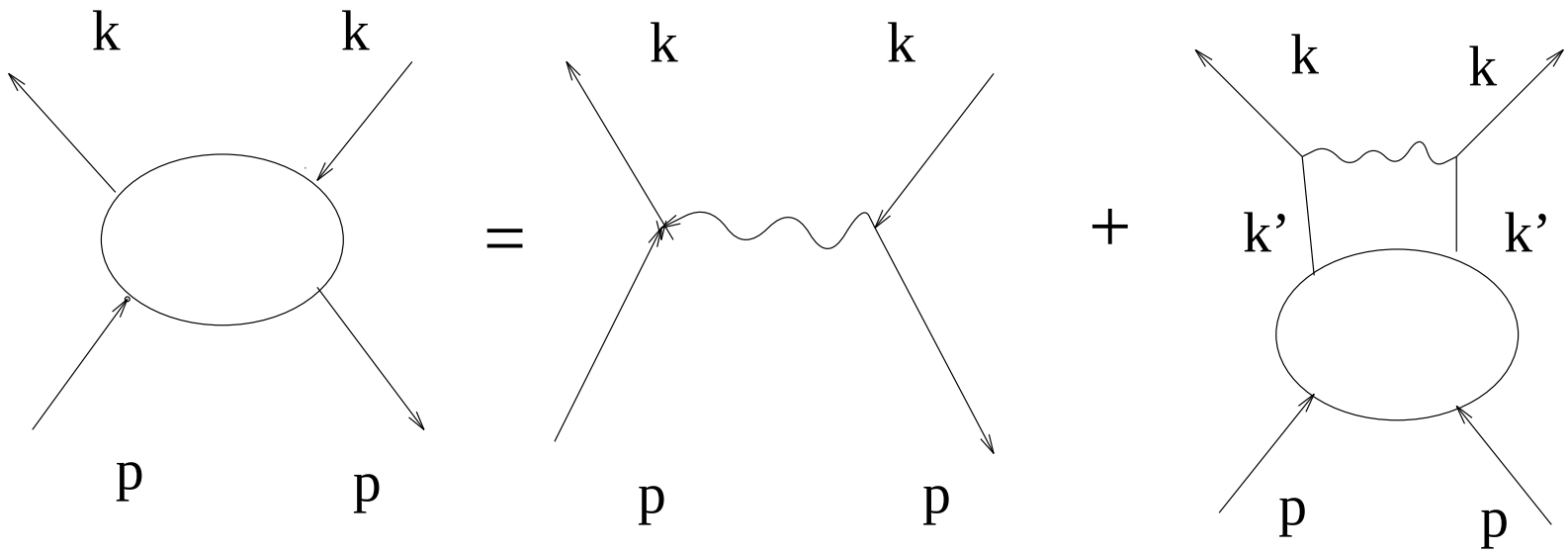

Fig. 3

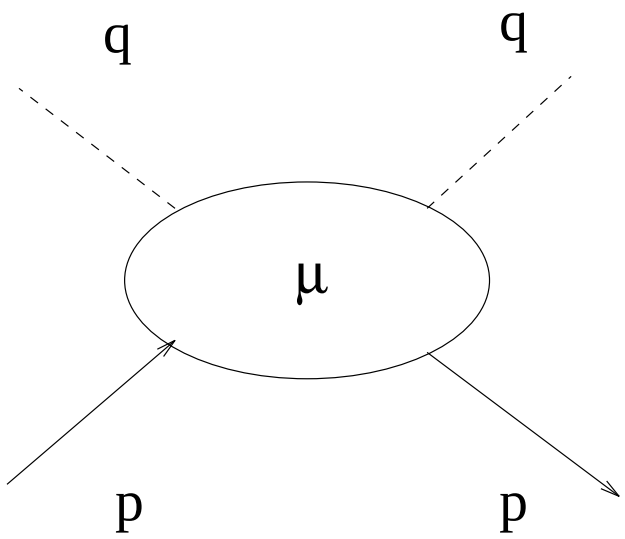

Fig. 4

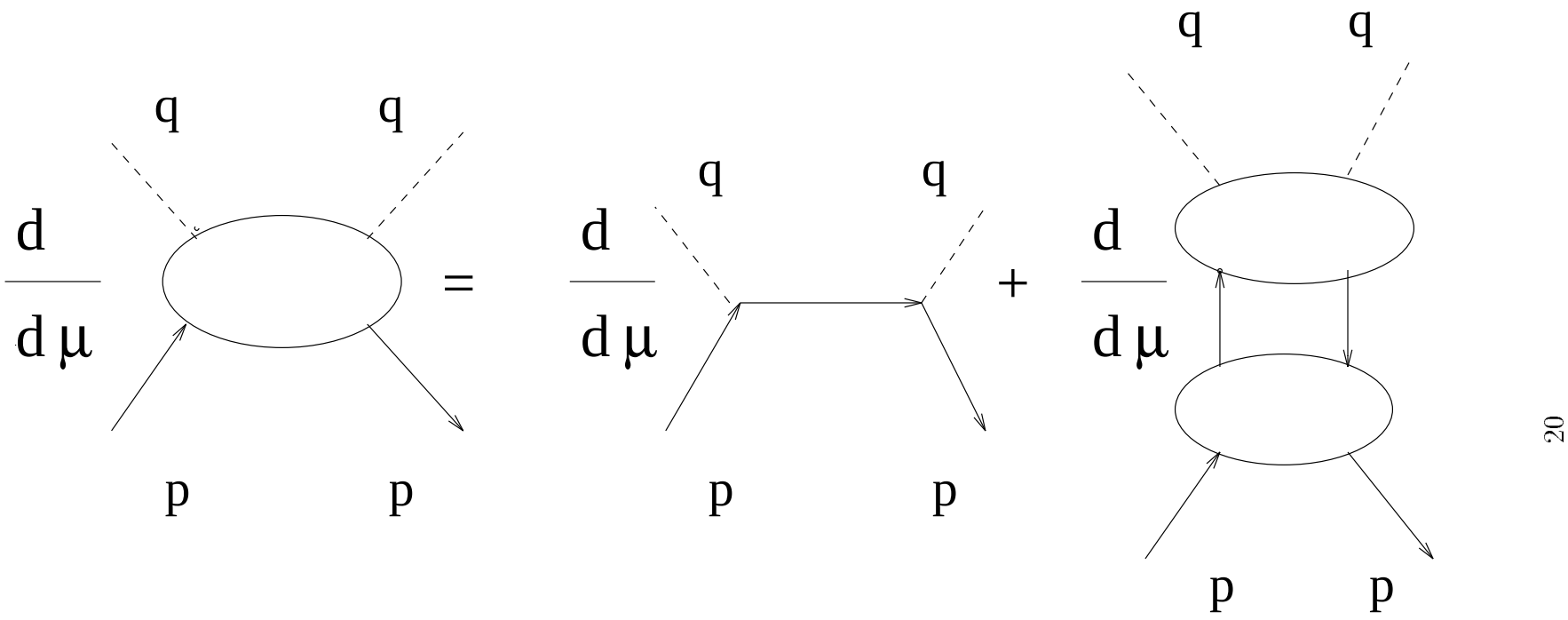

Fig. 5

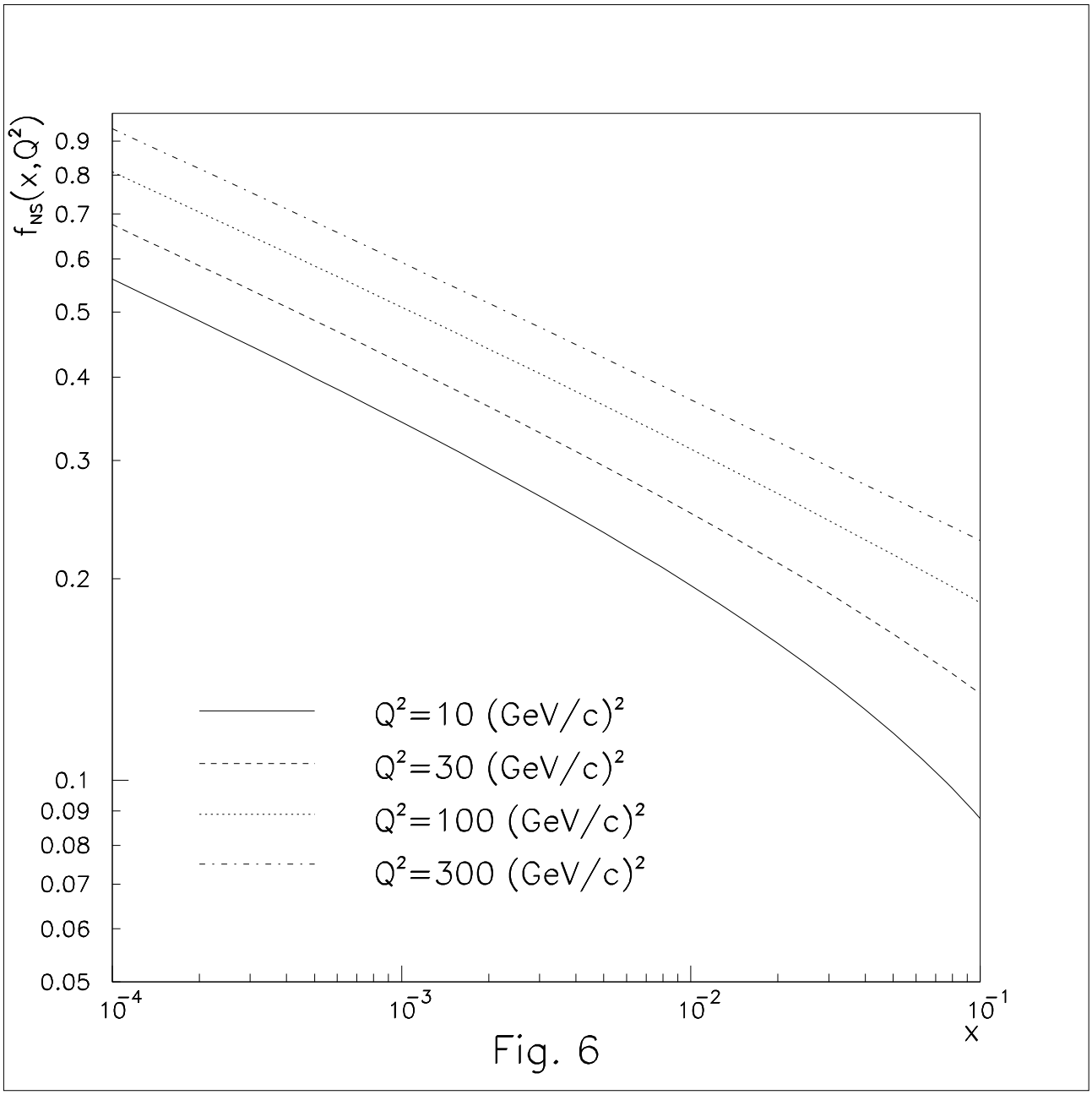
$f_{NS}(x,Q^2)$
0.9
0.8
0.7
0.6
0.5
0.4
0.3
0.2
0.1
0.09
0.08
0.07
0.06
0.05
10^{-4}
10^{-3}
10^{-2}
10^{-1}
x
Q^2=10 (GeV/c)²
Q^2=30 (GeV/c)²
Q^2=100 (GeV/c)²
Q^2=300 (GeV/c)²

Fig. 6

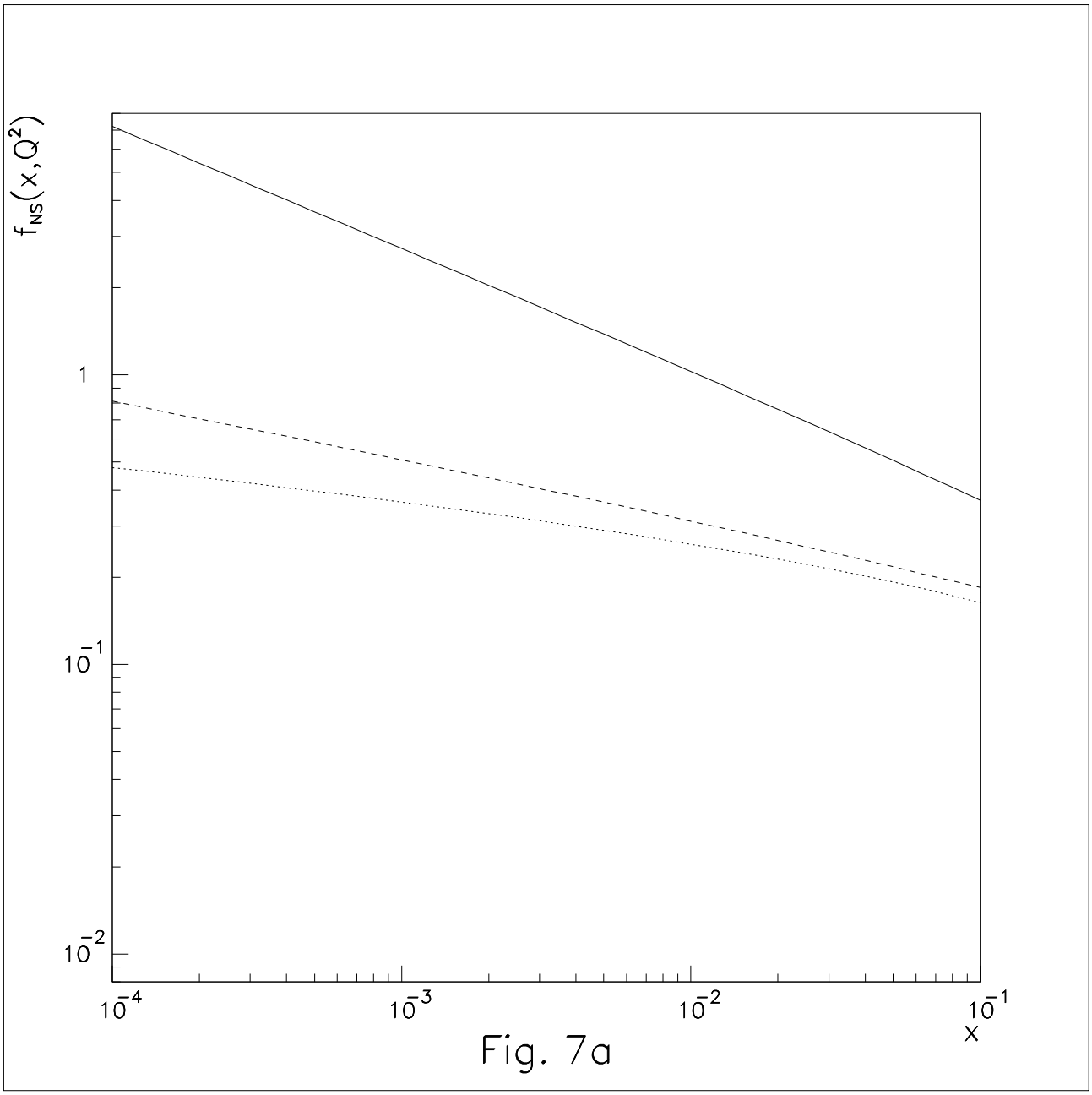

Fig. 7a

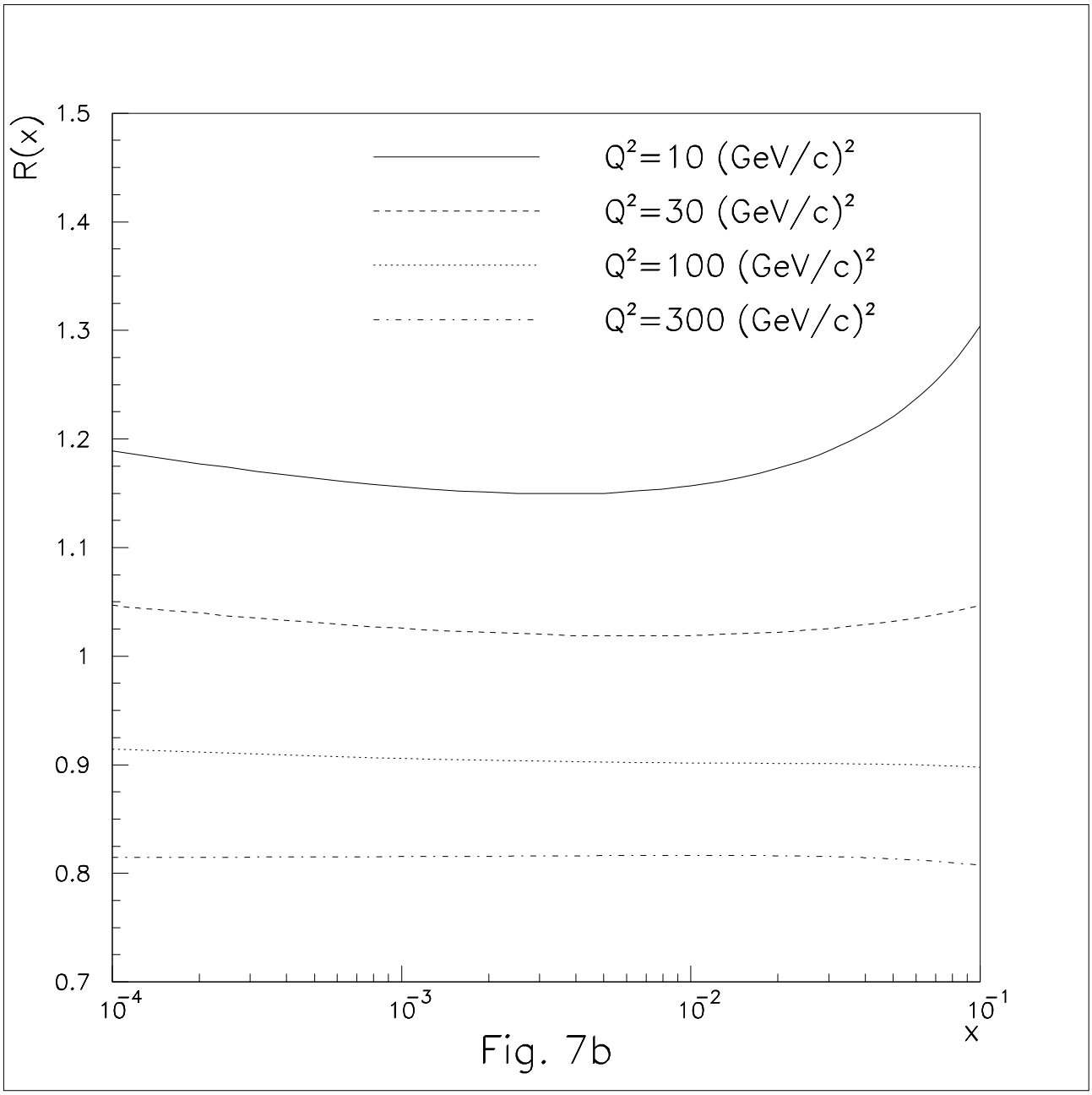
R(x)
1.5
1.4
1.3
1.2
1.1
1
0.9
0.8
0.7
Q^2=10 (GeV/c)^2
Q^2=30 (GeV/c)^2
Q^2=100 (GeV/c)^2
Q^2=300 (GeV/c)^2
10^{-4}
10^{-3}
10^{-2}
10^{-1}
x

Fig. 7b

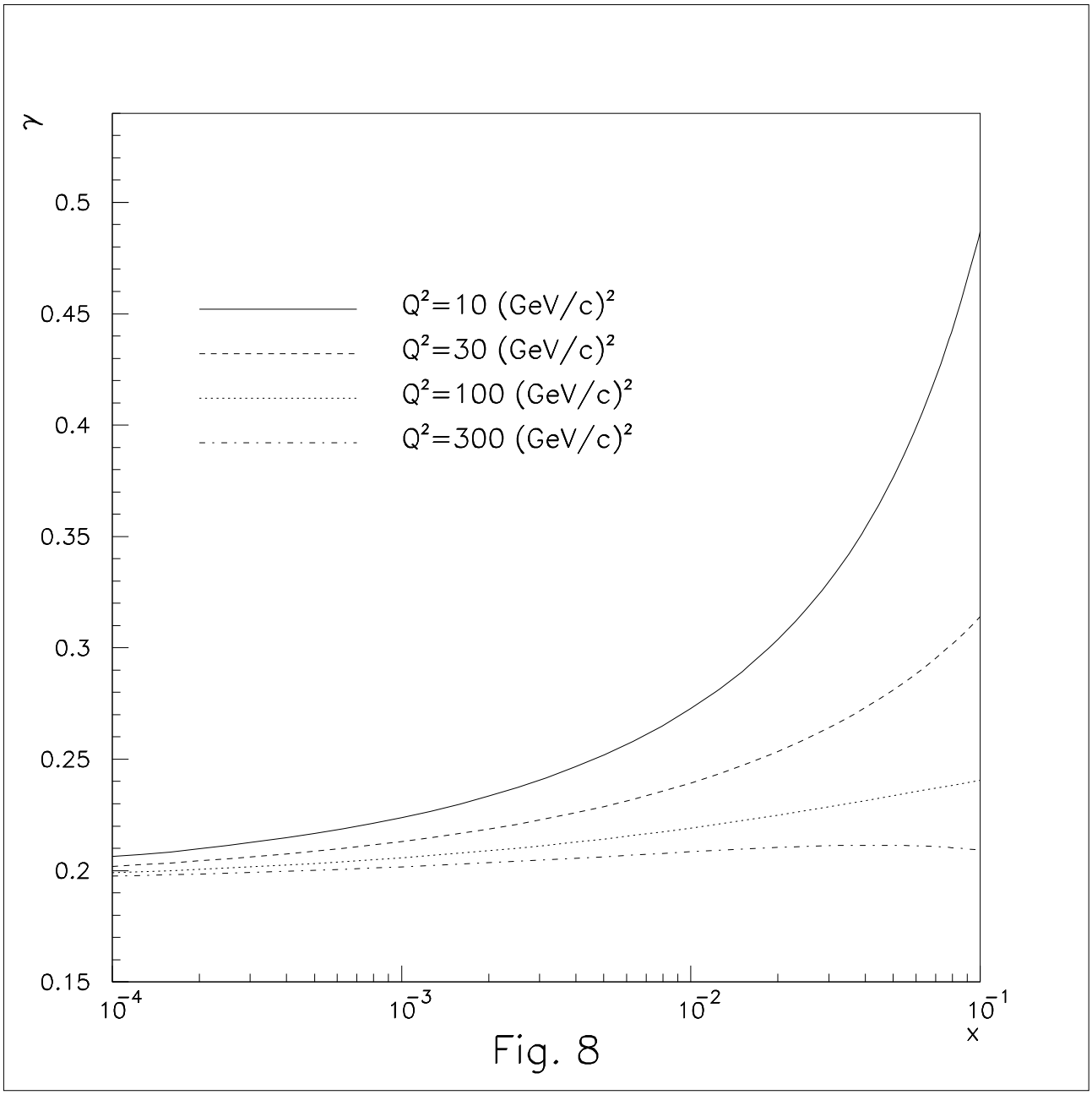
γ
0.5
0.45
0.4
0.35
0.3
0.25
0.2
0.15
Q²=10 (GeV/c)²
Q²=30 (GeV/c)²
Q²=100 (GeV/c)²
Q²=300 (GeV/c)²
10⁻⁴
10⁻³
10⁻²
10⁻¹
x

Fig. 8

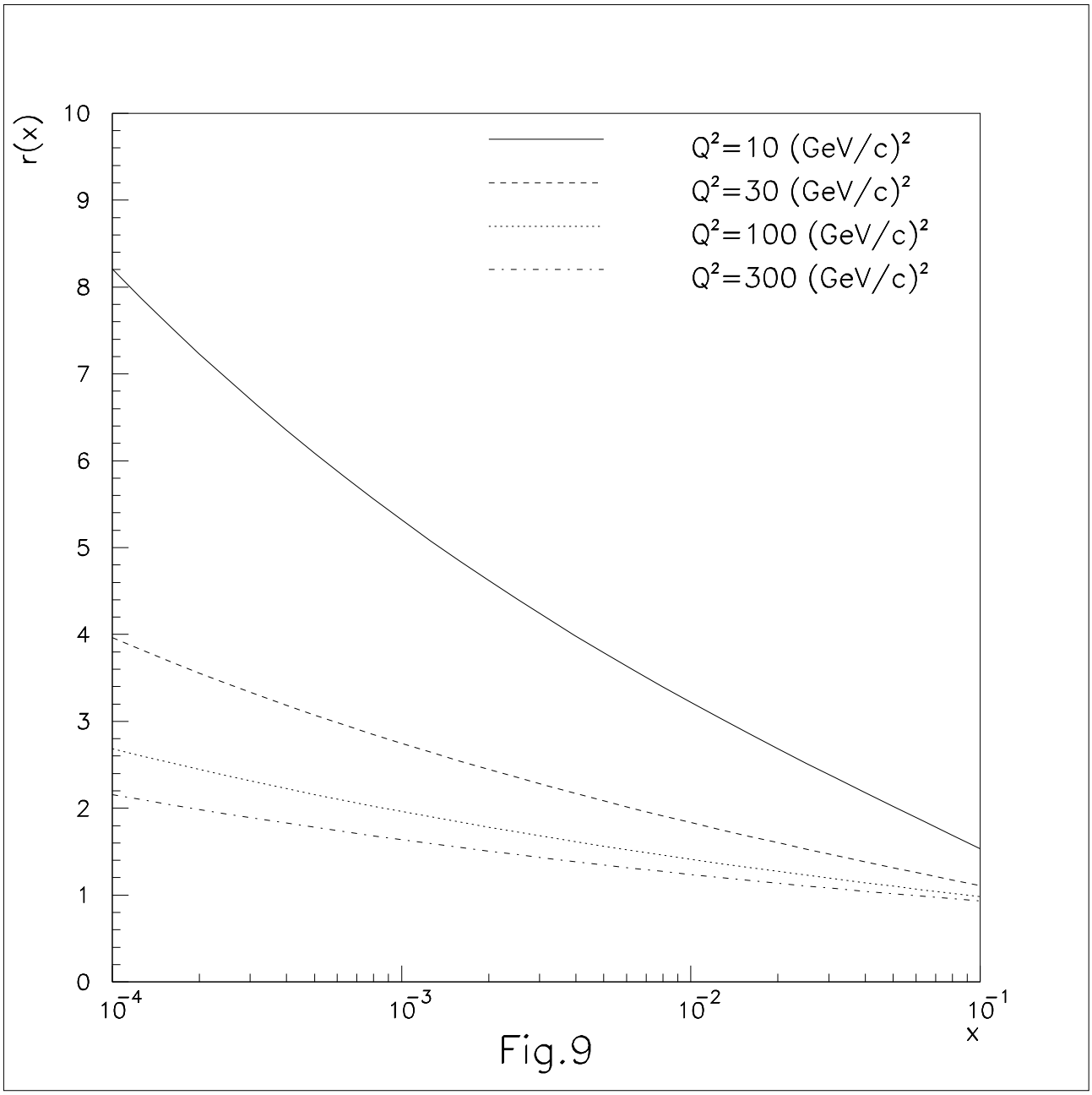
r(x)
10
9
8
7
6
5
4
3
2
1
0
10^{-4}
10^{-3}
10^{-2}
10^{-1}
x
$Q^2=10$ (GeV/c)^2
$Q^2=30$ (GeV/c)^2
$Q^2=100$ (GeV/c)^2
$Q^2=300$ (GeV/c)^2

Fig.9